Infusion Processing: An Alternative To Plasma Technology For Semiconductor Device Manufacturing

John Hautala, Wes Skinner, Steve Sherman, Yan Shao, & John Borland*
Epion Corporation, 37 Manning Rd., Billerica, MA, 01821
*J.O.B. Technologies, 5 Farrington Lane, South Hamilton, MA, 01982

Plasma technology, which is extensively used in the semiconductor industry is quickly reaching limitations. Rather than using plasma processing, we report on our studies using infusion processing for front-end-of-line (FEOL) and back-end-of-line (BEOL) semiconductor device manufacturing applications including: 1) photo resist strip and seal of ultra low k dielectrics 2) surface etching 3) surface doping and 4) thin film deposition. Conventional plasma processing can result in damage, poor across wafer uniformity and local-loading effects. Infusion processing using a gas cluster ion beam (GCIB) does not suffer from these effects because it uses an energetic neutral beam comprised of large clusters of atoms or molecules with only a few charges per cluster. The GCIB beam is rastered across the wafer and produces highly efficient localized process effects dependent on cluster chemistries, which we now describe as "infusion." New capabilities are described that can not be duplicated by conventional plasma techniques. For BEOL, the infusion process is used to strip photo resist and residues without damaging the ULK dielectric . For FEOL, infusion processing has produced ultra shallow junctions and offers the promise for doping with Ge to produce localized strain.

Infusion Processing Background

Gas cluster ion beam (GCIB) infusion processing is a novel method of treating surfaces in which a beam of high energy (1–30 keV) atomic or molecular clusters (n>5000) is incident on a surface. This contrasts to the monomer ions (defined here as an atomic or low molecular weight ions) used in the vast majority of semiconductor vacuum processes such as ion implant, plasma etch, and deposition. The physical processes underlying monomer ion interactions with materials are well understood over multiple orders of magnitude from <100 eV/monomer ion to >MeV/monomer. In the GCIB process, the cluster kinetic energy is shared among several thousand loosely bound atoms or molecules which results in a dramatically different physical processes when the cluster interacts with a surface. More recently Epion Corporation has reported cluster ion beam currents of 100 to 1000 microAmps formed of both inert gases such as argon and reactive gases including CF_4, NF_3, BF_3, SF_6, O_2, N_2, and CH_4 [2] and has released a fully automated 300-mm wafer processing tool incorporating these cluster ion sources (Figure 1). A mA/cm^2 beam consisting of 5000 atoms/cluster scanned over a 300 mm wafer delivers an energetic atom average flux equivalent to ~7mA/cm^2. A typical high-density plasma etcher would deliver an ion current of similar magnitude. As a manufacturing process technology, GCIB has now reached a level of maturity and productivity where

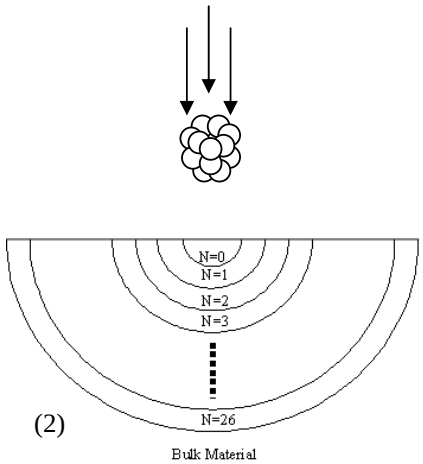

Figure 1. Depiction of infusion transient thermal spike emanating from cluster impact point

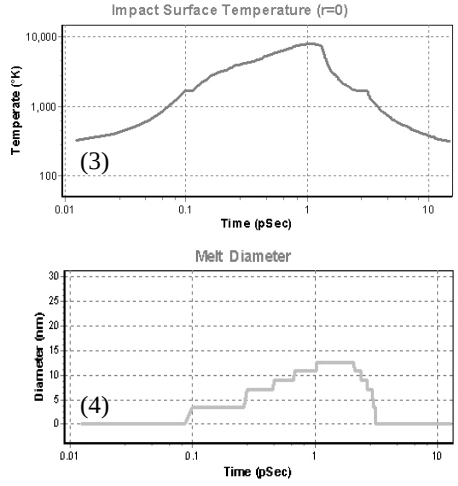

Figure 2. Time/temperature dependence of transient thermal spike

practical applications of the unique attributes of GCIB are feasible.

Cluster impacts differ significantly from single ion impacts on a surface. When a gas cluster ion strikes a surface, it produces a highly localized transient thermal and pressure spike (TTPS) lasting only a few picoseconds. This short timescale allows for thousands, or even millions of cluster impacts at a particular spot on the sample per second, each impact completely independent of the next. The volume of material in the substrate affected by a single cluster bombardment is linearly proportional to its energy and thus the depth to which a GCIB can affect any surface follows an energy to the 1/3 power dependence. This volume can be altered physically or chemically, or volatilized and pumped away depending on the constituents in the cluster and the material properties of the substrate. Variations in the GCIB process parameters alter these highly surface specific processes in which evaporation, sputtering, chemical alterations and shallow doping may all occur simultaneously.

Infusion processing for BEOL applications

The international technology roadmap for semiconductors (ITRS) requires low-k ($k<2.5$) dielectric materials to be implemented for interconnect technology at the 45nm node (1). Porosity is one method commonly used to lower the dielectric constant (k) of materials. Due to the porous and unique characteristics of ultra low-k films, the etch and ash processes must be developed to minimize damage, undesired film removal, and composition changes, as well as, moisture, ALD barrier precursor, and copper penetration. A method is needed for sealing porous sidewall features in order to protect the ultra low-k dielectrics from damage.

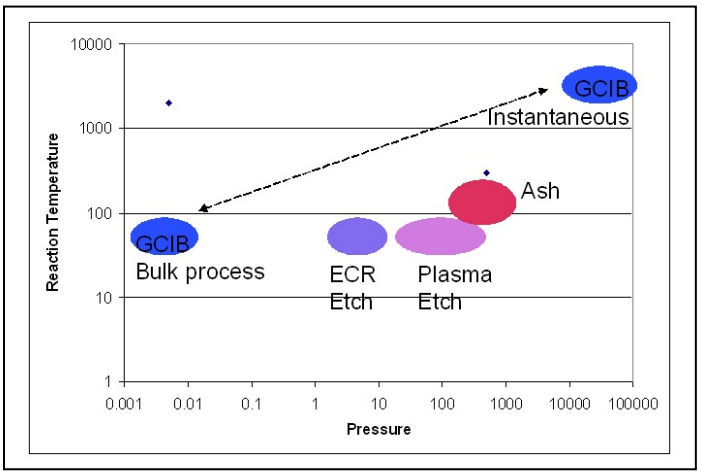

Conventional plasma processing can result in damage of thin gate oxides(2), notching(3), sidewall bowing, and aspect ratio dependent etching(4). Also, with the industry moving towards 300mm wafers, and as feature sizes shrink, etch and ash process uniformity and micro-loading must be minimized. GCIB is for a good candidate process for pore sealing, etching, and ashing of porous low-k films.

There are several potentially advantageous attributes of GCIB in semiconductor processing : (1) reactive species are only generated at the point of cluster/surface interaction, limiting the potential for undesired side reactions. (2) the cluster has typically 1-3 charges per >5000 atom cluster, hence charging effects are reduced by orders of magnitude relative to plasma processes with high degrees of ionization, (3) the beam is highly directional and allows for nearly 100% anisotropic processing for preserving CDs, (4) low processing pressures on the order of 10-5 Torr allow for long mean free paths and good by-product removal, (6) chemical reactions take place at room temperature processing, (7) no UV radiation is present, and (8) very small amounts of gases are needed due to the highly efficient cluster-surface interactions.

GCIB Evaluation on Low-k films

One application of GCIB in which these attributes offer advantages is shown if Fig. 2. Here the cluster beam is used to densify and seal the pores of the low-k dielectric without modifying its bulk properties either through absorption or intercolation of reactants and contaminants, or chemical modification of its backbone. The open, porous microstructure of potential intermetal dielectrics with k-values < ~2.5, and their low atomic density lead to several problems when fully integrated with Cu metallization. These include fluorine intercolation during etch or ash, leading to subsequent voiding of the low-k, resist poisoning from NH_3 desorption, and H penetration, or reaction of the low-k backbone with reactive species

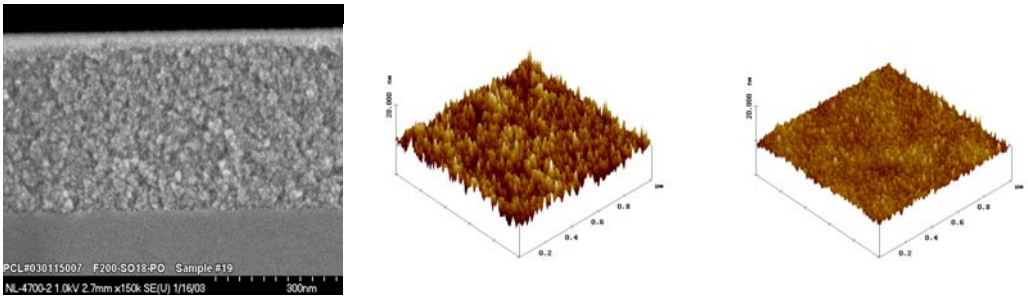

Figure 2. Example of a Cluster Beam Densified (CBD) layer of a porous low k. A SEM cross section image (a), and a pre (b) and post (c) GCIB processed surface measured by AFM.

generated in plasmas or CVD processes. Here we report initial results of integration of a GCIB-based pore sealing and combined photoresist ash-pore seal process. Argon GCIB processing on porous low-k materials at ISMT was investigated on blanket spin-on methyl-silsesquioxane (p-MSQ) films of k~2.2 on 200mm Si wafers. These results showed that GCIB densified and sealed the low-k surface preventing Ti penetration of a PECVD TiSiN film, which was deposited on the surface, see fig. 1. The untreated sample showed Ti penetration with the same film deposition conditions.

Both blanket films and damascene trench structures were studied. Blanket films evaluated for pore sealing consisted of 200-400 nm JSR-5109 on silicon. Integration issues and combined ash/pore seal processes were evaluated on 0.25 um single damascene trench structures. The reticle contains features suitable for cross section SEM analysis and, with addition of barrier, seed , Cu ECD and CMP contains a full set of features for characterization of metal and low-k integration issues.

In order to integrate Cu and low-k by implementing GCIB pore sealing; however, it would be necessary to densify not only surfaces in the field (normal incidence), but surfaces such as via and trench sidewalls which present an oblique angle of incidence to cluster directed parallel to the wafer surface normal. The effect of angle of incidence on CBD layer thickness is shown in Figure 3(b) for an Ar 30kV beam. In order to achieve oblique incidence blanket thin film samples were mounted in a jig at varying angles, thus allowing CBD layer thickness to be measured by SE using the same modeling approach. Even at the high angles relative to the local surface normal as would be characteristic of grazing incidence on trench or via sidewalls a substantial CBD layer is formed. A 4:1 aspect ratio feature requires an angle of incidence of approximately 75 degree, at which point a CBD layer thickness of approximately 10 nm results, indicating the fundamental feasibility of applying GCIB to pore sealing of moderate aspect ratio structures.

GCIB Low-k Ash Results

Blanket film studies are important to answer some basic feasibility questions, but do not address the full complexity of an integrated process flow in which barriers, seed layers, and Cu ECD must be combined with low-k patterning. The kinetic nature of the GCIB process together with the fact that reactive byproducts are only formed at the point of impact open new process possibilities. Introduction of O_2 into the cluster source leads to generation of oxygen-containing clusters. These clusters can be either 100% oxygen or a mix of oxygen and other gases. Based on molecular dynamics modeling and experience in other materials systems it is expected that on impact with the surface the oxygen present in the cluster can be activated as the cluster disintigrates. In addition the large kinetic energy of the cluster creates a short, highly non-equilibrium shock in the photoresist, promoting reaction with the photoresist polymers and formation of volatile reaction by products. In this case the kinetic energy of the cluster impact replaces the thermal energy and plasma activation present in conventional ashers. In contrast, however, very few charged species are present and any radicals generated react within the near surface region.
One attractive option presented by GCIB would be to utilize an oxygen containing beam to both ash photoresist while simultaneously sealing low-k pores on sidewalls. From Figure 3 it can be seen that O_2 beams will also create a CBD layer at the porous low-k surface. The same beam conditions are sufficient to ash photoresist at effective etch rates of >100 nm/min for 200 mm wafers. Several “short loop” experiments to investigate various aspect of integrating a combined ash/seal step have been performed in which GCIB

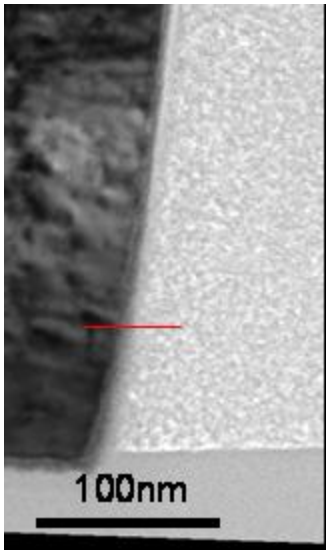

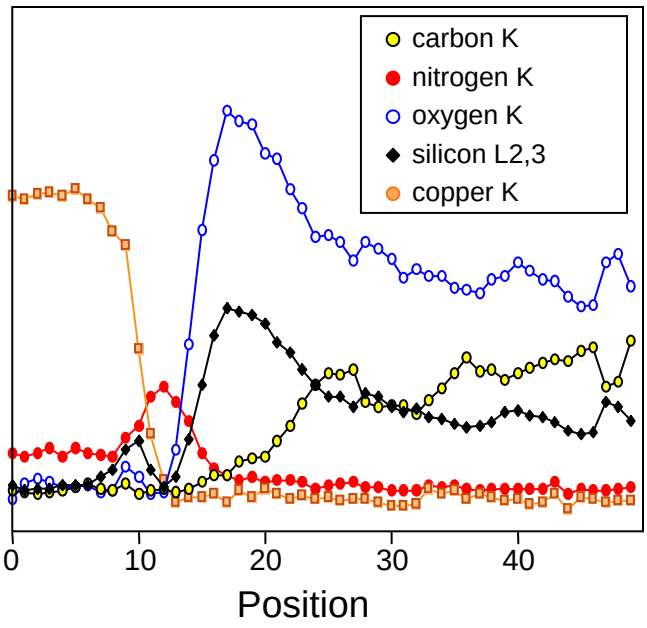

processes have been integrated into Sematech's standard Cu/low-k dual damascene flow.

For the ash evaluation and electrical test results, the low-k single damascene stack consists of 400nm p-MSQ dielectric sandwiched between 100nm of plasma enhanced chemical vapor deposited (PECVD) SiCN. Patterning of the 250 nm line and 300 nm space features was performed on 600nm thick 248nm (KrF) photo resist on 60nm BARC. The dielectric stack is etched in a magnetically enhanced reactive ion etch (RIE) chamber, utilizing $C_4F_8/Ar/N_2$ chemistry. The ISMT process of record (POR) ash split is done in a separate RIE chamber with an N_2/H_2 chemistry. The post etch resist removal (ash) splits were performed with the GCIB processing at Epion. The wafers were integrated with 25nm PVD Ta copper barrier, 800nm Cu electroplate, 150°C Cu anneal, Cu CMP, and SiCN/oxide/nitride passivation deposition.

The GCIB ashing experiments on 200mm p-MSQ wafers were done using oxygen and nitrogen/oxygen chemistries. These ash tests were performed with a 5° off normal incidence process and 10° off normal GCIB process, see fig. 3. The 10° off normal GCIB process are more desirable for patterned features in order to maximize the GCIB effect on the low-k sidewall. The beam conditions for this test were 30kV energy and 1.6E15 dose. The pore sealing ability of GCIB was tested on a normal oxygen beam ashed sample with PECVD TiSiN deposition. TEM and EELS analysis was done to investigate any Ti penetration into the low-k, see fig. 4. The EELS analysis shows no Ti penetration at the top of the feature sidewall.

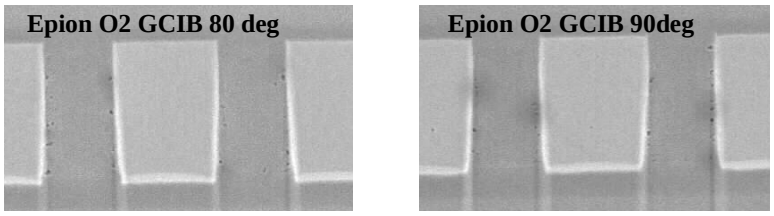

Figure 5 Post 96hr bake at 250C on passivated GCIB ashed wafers. Only minor low-k voiding is observed on the 0.25/0.30 micron features.

Full wafers with p-MSQ single damascene test structures were ashed using oxygen GCIB at normal and 10° off normal processing. The passivated samples were baked at 250°C for 96 hours at ambient conditions and cross-sectioned, see fig. 5. A structure surrounded by a Cu seal was chosen for the SEM sample. Only minor low-k voiding is observed and the feature profiles are consistent with the ISMT POR ash process (8).

Electrical Data – GCIB Ash

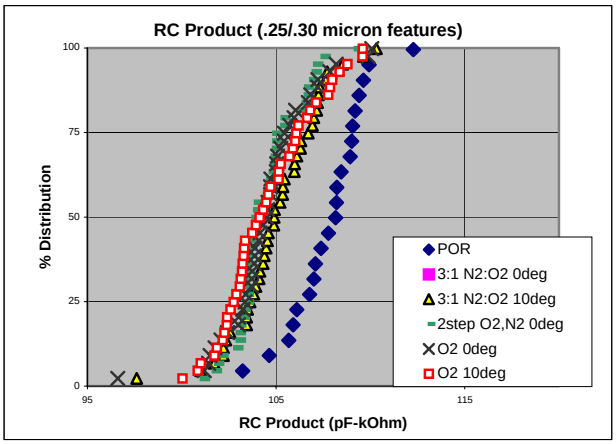

Figure 6 RC product distributions comparing the GCIB ash splits to the ISMT POR ash process.

Single damascene copper and p-MSQ serpentine and comb structures were electrical tested to investigate the low-k damage caused by the GCIB ash processes was compared to the ISMT POR ash process. The 200mm wafers were passivated and annealed at 400°C before collecting RC product data, which is used to estimate k_{eff}, see fig. 6. RC products for the GCIB splits give comparable data to the ISMT POR ash process. Voltage ramp of the 0.25/0.30 micron structures on full wafers was also performed to compare the dielectric breakdown field strength between the splits. From table 1, the breakdown field for the ISMT POR ash process is the highest, but two GCIB ash splits give good breakdown field results, the 3:1 N_2:H_2 10° split and the O_2 only split at 10°. There is a significant difference between the angled O_2 GCIB ash split and the normal beam O2 ash split, with the angled GCIB ash split having nearly a 2 times higher breakdown field strength. These results are very encouraging since it is possible for an angled GCIB ash process to pore seal the low-k feature sidewalls and protect the inter-layer dielectric from damage.

GCIB Low-k Etch Results

The ability of GCIB to etch SiC and p-MSQ was evaluated. Partially etched samples were sent to Epion for GCIB etching of the cap and p-MSQ layers. This test was done on 300mm wafers at ISMT, with ArF lithography on 400nm of 193nm photo resist and 80nm of BARC with 125nm wide features as printed. The rest of the film stack consisted of 70nm of SiC cap, 200nm k=2.2 p-MSQ low-k film, and 100nm SiC etchstop. A gas combination of 5% NF_3 and oxygen was used for the GCIB etching tests.

The ability of GCIB to etch features was performed on single damascene structures. For the initial GCIB etch tests, the 80nm BARC layer was etched at ISMT. Wafers were etched under several beam conditions, see fig. 2.

Figure 3 Post etch and oxygen GCIB ash cross sections showing good profiles and vertical profiles for 5° and 10° off normal processes.

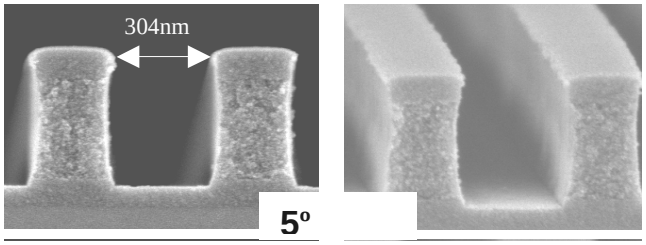

Two different process conditions were used for low-k feature etching. Depending on beam conditions, the resist:SiC selectivity was found to be as high as 1.6:1 (process A) and as low as 0.7:1 (process B). The micro loading between 3:1 aspect ratio, 125nm wide features, and 1:1 aspect ratio, 500nm wide features was found to be about 10%. Experimentation is ongoing for the GCIB low-k etch process.

Conclusions

In this work we show how GCIB processing is able to etch, ash and pore seal ultra low-k dielectric samples. From physical SEM data and electrical data, it can be concluded that GCIB ash processing is compatible with porous low-k films, causing no additional film damage when compared to standard RIE

etch and ash processes. The pore sealing ability of the GCIB process is evident from this data, but must be further developed for optimized results.

References

[1] International Technology Roadmap for Semiconductors, Semiconductor Industry Association, San Jose, CA (2003).
[2] C.T. Gabriel and J.P. McVittie, *Solid State Tech*. **35(6)**, 81 (1992).
[3] N. Fujiwara, T. Maruyama, and M. Yoneda, Jpn. *J. Appl. Phys*. **35**, 2450 (1996).
[4] R.A. Gottscho, C. W. Jurgensen, and D.J. Vitkavage, *J. Vac. Sci. Technol. B*, **10**, 2133 (1992).
[5] I. Yamada, *Radiation Effects in Solids*, **124**, (1992) 227.
[6] W. K. Chu et. al., Appl. Phys. Letters, **72**, (1998) 246.
[7] B. White et. al., Proceedings of the IITC, p 153 (2003).
[8] T. Jacobs et. al., Proceedings of the IITC, p 236 (2002).

USJ FORMATION

The generally accepted USJ requirements for the 45 nm node include a doping depth of 10 nm, <0.1% energy contamination, and diffusion-less activation. Infusion processing with GCIB addresses all of these concerns. Although the gas cluster ions have high total energy, the energy is shared by the large number of atoms comprising the cluster, so that the energy per atom is <10eV. Upon impact with the silicon surface, the atoms in the gas cluster are only able to be penetrate through a few atomic layers of the surface, because of the low energy per atom. This is much shallower than in the case of conventional ion implantation and allows processing effects to be confined to much shallower depths. The high total energy of the cluster ion is infused into a very small region of the silicon surface resulting in momentary surface temperature and pressure conditions which are significantly higher than those produced by conventional ion processes. Unlike ion implantation, the stopping distance for infusion doping follows the energy of acceleration to the 1/3 power. This is because upon impact with the substrate, the cluster locally heats a volume of Si by a transient thermal spike (TTS). At the instant of contact with the cluster, the solids incorporated in the cluster are infused into this heated/pressurized zone. The TTS propagates in 3-dimensions and is quickly quenched.

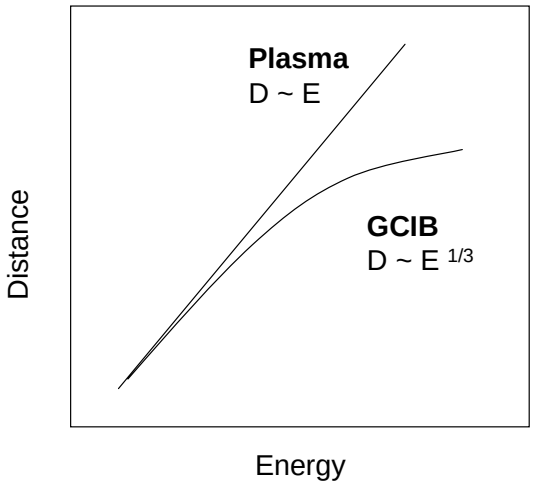

Figure 5: Infusion depth vs. GCIB energy for 1E15/cm^2 B doping.

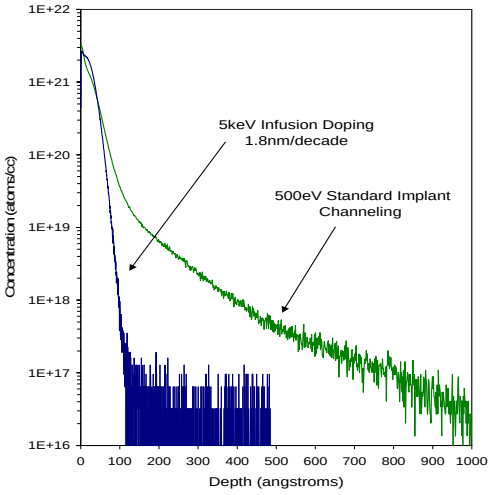

Fi

Figure 3: Infusion 5 keV 1E15/cm2 boron doping vs traditional 1E15/cm2 beam line

Figure 5 shows the energy to 1/3 power law of the GCIB doping process over the same energy range. Activation behavior of the B for this type of infusion doping appears to be very similar to traditional beam line implanted boron. Furnace, spike and flash anneals all show activation levels similar as those reported by traditional implantation. Figure 3 shows a comparison between traditional 500 eV B_{11} monomer ion implantation doping and infusion doping by 5 keV gas clusters made up of a mixture of B_2H_6 and Ar gases. No channeling is observed using the infusion doping technique and a 1E18/cm^3 junction depth (Xj) at 9.7 nm is achieved with an extreme abruptness of <1.8 nm/decade. Significant channeling can be seen with the ion implantation process resulting in an Xj at 37 nm. Since the individual B atoms in the gas clusters have <10 eV of energy, no channeling or energy contamination is possible, and the depth to which the B atoms penetrate into the Si surface is only determined by the collective energy of the cluster. Since no channeling or energy contamination exists, then either a pre or post Ge/Si amorphizing step can be used to promote diffusion-less activation. Figure 6 shows the

SIMS and SRP profile of 5keV GCIB infusion of 2E15/cm^2 boron that then had a post 5E14 5 keV standard beam line Ge implantation. Being fully amorphous, this process required only the SPE furnace anneal of 1 hour at 550°C. This combination of GCIB infusion and post amorphization with traditional beam line Ge and SPE anneal resulted in an extremely shallow 6 nm junction with >1E20 /cm^3 boron activation.

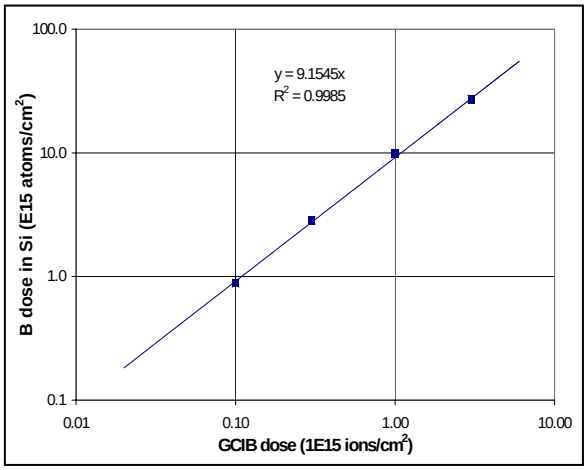

The doping rates are controlled by the GCIB energy and by the gas mixture ratio. A one-to-one correlation between the gas cluster dose and the SIMS measured retained boron dose in silicon is strictly maintained [1]. The number of B atoms infused into the Si is linearly proportional to the GCIB energy and > 200 infused B atoms per gas cluster is possible, allowing for highly efficient doping processes.

SELF-AMORPHIZING USJ

Adding GeH_4 gas to the $Ar+B_2H_6$ gas clusters results in self-amorphization of the USJ structure without requiring the additional Ge pre-amorphizing implantation (Ge-PAI) step usually used in traditional implantation for diffusionless activation of USJ. The Ge naturally infuses to the same depth as the B and doping level is controlled in the same way as the B, namely by gas mix concentration and GCIB dose. A SIMS profile of a self-amorphizing process is shown in Figure 8. This ability saves one process step for USJ formation, which is significant, but much more importantly, the self-amorphizing infusion doping produces no evidence of End of Range (EOR) damage (Figure 9). This is understandable since the mechanism for the infusion of the Ge is entirely distinct from implanted Ge, which causes excess interstitials beyond the amorphous interface as reported by Matsuda et al. [13] and shown in Figure 10.

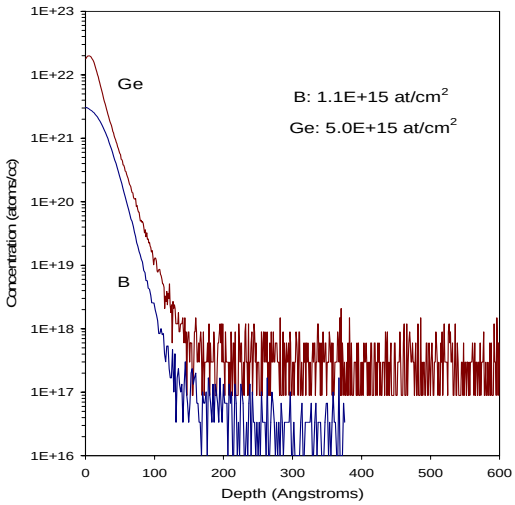

Figure 8. SIMS profile of simultaneous Ge and B infusion for self-amorphization.

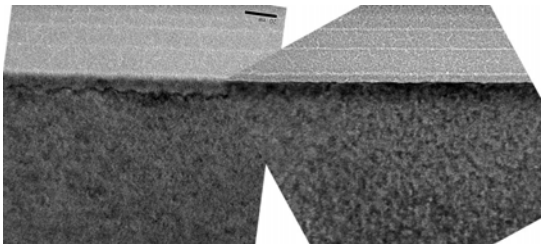

Figure 9. Self-amorphizing B/Ge infusion (left) and single crystal SiGe with no EOR after SPE anneal (right).

The self-amorphous SiGeB structure is shown in Figure 11. After either a 550°C or 950°C 1 hour anneal, complete SPE recrystallization is observed. No residual defects were observed by planar or cross-sectional TEM. Thus GCIB enables a simple methodology for the formation of diffusionless USJ with the important benefit

of no observed EOR, which in turn should appreciably reduce leakage. This process should be compatible with all the major annealing methods used for SPE activation.

LOCALIZED STRAINED-Si

The SiGe material system has received much attention in the last few years as being critical to continued device scaling and extending the life of planar single gate CMOS technology. SiGe epitaxy provides two unique and independent benefits for CMOS device scaling: increased boron solid solubility (Bss), and device channel mobility enhancement using strain-Si. To incorporate this into pMOS devices would require selective etching laterally under the gate edge followed by SiGeB selective epi growth (SEG) as reported by Ozturk et al. [14] and Mansoori [15].

As with any SEG process, surface cleaning to eliminate epi/substrate interface contamination is very critical. This is followed by a very costly and complex process involving multiple thick and thin SiGe and Si epitaxial deposition and cleaning steps. Misfit dislocation at the epi/substrate interface and 10^5 to 10^7 defects/cm^2 on the top epi layer surface are typical. There has been debate over what is the preferred strain method, global blanket biaxial strain-Si epi on relaxed SiGe epi or to have localized tensile and compressive strain. Localized uniaxial tensile strain in the channel for nMOS devices while localized uniaxial compressive strain in the channel for pMOS devices was reported by Ghani et al. of Intel using localized selective SiGeB SEG process for pMOS to induce uniaxial compressive strain in the channel [16].

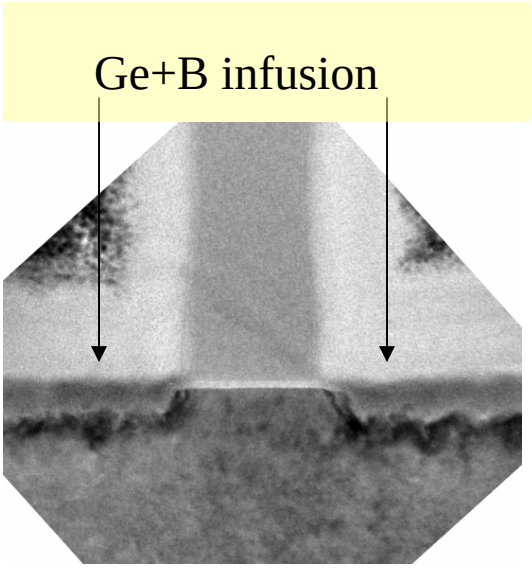

Figure 13. High level Ge and B S/D infusion for localized high strain-Si

As an alternative to using SiGe epitaxial growth or high dose Ge ion implantation, Ge infusion can be used to form localized or blanket SiGe and Ge structures. This technique can eliminate the complex process of depositing a thick graded layer and then relaxed SiGe epitaxial layers followed by a post polishing step for blanket SiGe formation for bulk CMOS. For PD/SOI CMOS applications this technique can be used with either SIMOX or bonded SOI wafers and can potentially reduce the processing steps by up to 75%.

The strain is controlled by the Ge concentration, the depth of the SiGex layer is controlled by the GCIB energy. For the high strain in the shallow source drain extensions, more Ge is infused (up to 100% on the surface) than what is shown in Figure 8. Making high strain deeper source/drains requires higher energy GCIB infusion: in either case high concentrations of Ge and B are possible without going into deposition as shown in Figure 13. Thus infusion represents a simple method for producing either blanket strain-Si as compared to the costly epi + CMP process or

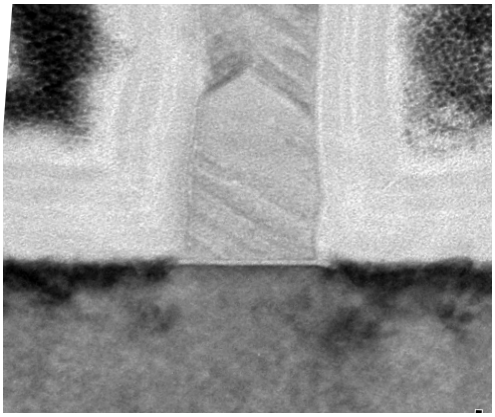

Figure 14. Localized high strain-Si with Ge/B infusion. As infused amorphous SiGeB (top), and after SPE anneal showing good crystalline re-growth (bottom).

localized strain-Si as compared to the complex isotropic etch + selective epi (Figure 12). The simple simultaneous Ge+B infusion formation of a highly strained source/drain extension is shown in Figure 14. These TEMs demonstrate the infusion of Ge+B+Ar clusters is essentially 100% anisotropic and with no evidence of interaction with the sidewall of the poly Si. A completely amorphous SiGeB layer is formed that contains a strongly graded Ge concentration. After a SPE anneal, single crystal heavily doped SiGe is formed. Unlike traditional epi, the infusion process appears to be insensitive to the quality of the original Si interface, where perfect crystallinity with low defect density is attained even with un-cleaned Si. This is likely due to the unique aspect of having no true interface, but rather a 10 to 30 nm deep infusion and concentration gradient of all species present (including surface oxide) into the sub-surface amorphous layer. Concentrations up to and including 100% Ge are possible by this method with no evidence of the misfit and strain defects observed by CVD methods where the defects mostly originate from the Si interface. Raman (Figure 15) and plan view TEM analysis (Figure 16) also show no evidence of the strain relief cross hatching always observed with the CVD SiGex.

Substituting a C-containing gas such as CH_4 for the GeH_4 similarly results in infusing C into the surface of Si. This will result in a controllable method of compressive strain layers for enhanced nMOS channel mobilities.

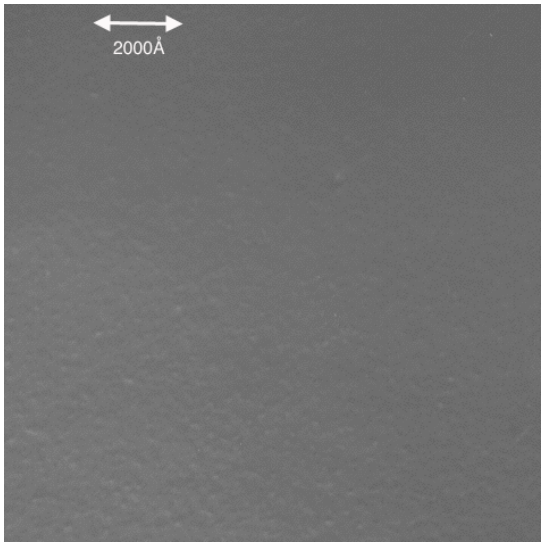

Figure 16. Plan view TEM of Ge infused Si with >50% Ge on surface. No strain relief roughness is observed. Inset shows good single crystal by electron diffraction.

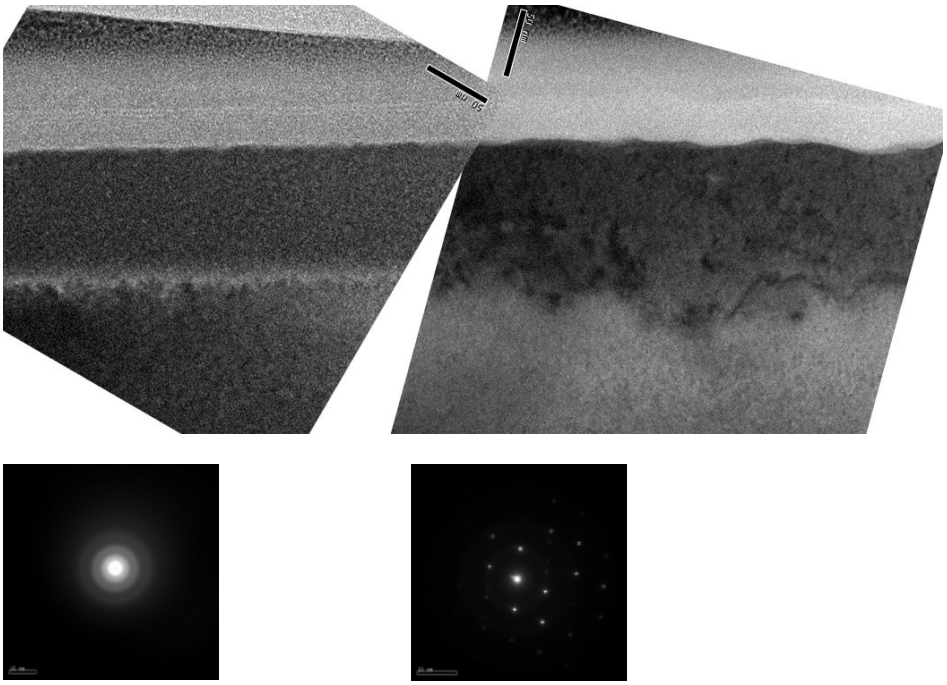

Figure 17. Cross section TEMs of 20 nm Ge infusion + 90 nm amorphous Ge deposition. Electron diffraction patterns are also shown for as-infused (left) and after 950°C anneal (right).

INFUSION DOSE CONTROLLED DEPOSITION (DCD)

Continuing the process after infusing Si with

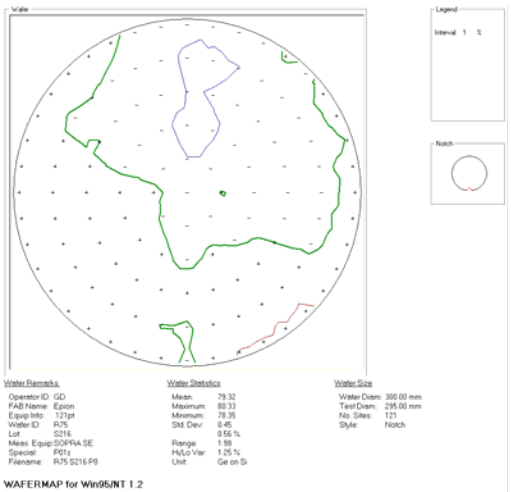

Figure 19. Elipsometry map of 70 nm infusion Dose Controlled Deposition (DCD) of amorphous Ge.

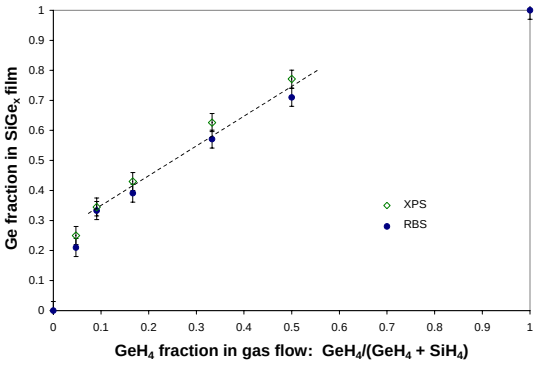

Figure 18. Ge fraction vs. gas mixture for infusion deposition of SiGex. A linear response is observed for 30 to 80% Ge fraction films.

sufficient Ge such that 100% Ge is attained on the surface, deposition of amorphous Ge begins. The deposition thickness is directly controlled by the GCIB dose. Controllable ranges of the Ge/B/Si ratios are easily managed by the gas mix and beam conditions. The TEM results for a 90 nm deposited amorphous Ge+B layer is shown in Figure 17. A few threading dislocations are now visible after the 950^{o}C anneal for this thick recrystallized Ge+B layer and electron diffraction pattern results are shown. By including SiH_4 in the gas mix, amorphous Si can also be infused and deposited. The full range of SiGex from amorphous Si to amorphous Ge can be controllably made by GCIB as shown in Figure 18. The scanning process is inherently controllable and allows for highly uniform depositions as shown in Figure 19. Since this is a room temperature process, it is compatible with photoresist. This opens up the possibility of a controllable low cost, low defect density, pure Ge channel engineering.

SUMMARY

USJ formation using infusion doping with boron achieved <10 nm junctions determined by SIMS with a 1/3 power log relationship with no evidence of channeling and abruptness of <1.8 nm/decade. Surface boron chemical doping levels as high as 2E22/cm^3 were achieved and box-like dopant profiles can be engineered. Infusion doping or deposition with Ge+B resulted in self-amorphization without the typical EOR damage after SPE recrystallization. At higher Ge doses, localized or blanket strained SiGeB can be manufactured. With yet higher doses of Ge, or Ge/Si mixes, dose controlled deposition of amorphous Ge of SiGex films are possible. This process is insensitive to surface native oxide enabling SPE single crystal regrowth at temperatures down to 550^{o}C without the typical misfit dislocation and high density of threading dislocation. The process takes place at room temperature and is compatible with photo resist patterning.

REFERENCES

[1]. J. Hautala, J. Borland, M. Tabat and W. Skinner, *IWJT-2004*, Shanghai, China p. 50, March 2004.

[2]. J. Borland, *et al*, Solid St. Tech., May 2004. p.53.[3]. B. White, G. Book, J. Hautala, M. Tabat, 2004 Int'l Interconnect Tech. Conf., IEEE, San Francisco
[4]. J. Hautala, *et al*, 2003 Advanced Metallization Conf., Montreal, Canada, p. 461

[5]. L. P. Allen, S. Caliendo, N. Hofmeester, E. Harrington, M. Walsh, M. Tabat, T. G. Tetreault, E. Degenkolb, C. Santeufemio and W. Skinner, *2002 IEEE International SOI Conference*, Williamsburg, VA, October 7-11 (2002).

[6]. M. Saito, N. Toyoda, N. Hagiwara, J. Matsuo and I. Yamada, *Ion Implantation Technology-98*, 1226, edited by J. Matsuo, G. Takaoka and I. Yamada, IEEE, Piscataway (1999)

[7]. N. Toyoda, J. Matsuo and I. Yamada, *Implantation Technology-96*, 808, edited by E. Ishida, S. Banerjee, S. Mehta, T. C. Smith, M. Current, L. Larson and A. Tasch, IEEE, Piscataway (1997)

[8]. M. E. Mack, R. Becker, M. Gwinn, D. R. Swenson, R. P. Torti and R. Roby, "Design Issues in Gas Cluster Ion Beamlines", *Ion Implantation Technology: IIT 2002 Proceedings* edited by B. Brown, T. L. Alford, M. Nastasi and M. C. Vella, 665, IEEE, New Jersey (2003)

[9]. J. Bachand, A. Freytsis, E. Harrington, N. Hofmeester, J. Hautala, M. E. Mack,

K. Regan, "Gas Cluster Ion Beam Processign Equipment", *Ion Implantation Technology: IIT 2002 Proceedings* edited by B. Brown, T. L. Alford, M. Nastasi and M. C. Vella, 669, IEEE, New

Jersey (2003)

[10]. D. R. Swenson, “Measurement of Averages of Charge, Energy and Mass of Large, Multiply Charged Cluster Ions Colliding with Ions”, Nucl. Inst. Methods B 222, 61 (2004)
[11]. M. Gwinn, M. Mack *Ion Implantation Technology: IIT 2004 Proceedings*. to be published

[12]. Quanming Lu, Samuel Mao, Xianglei Mao, Richard E Russo, “Delayed phase explosion during high-power nanosecond laser ablation of silicon”, Appl. Phy. Letters, Volume 80, Number 17 (2002)
[13]. T. Matsuda, *vTech/Japan 2002* presentation material, Dec. 2002.

[14]. M. Ozturk, N. Pesovic, J. Liu, H. Mo, I. Kang and S. Gannavaram, *Semiconductor Silicon 2002*, the Electrochemical Society, PV 2002-2, vol. 2, p. 761.
[15]. M. Mansoori, *vTech 2002* presentation material, July 2002.
[16]. T. Ghani, M. Armstrong, C. Auth, M. Bost, P. Charvat, G. Glass, T. Hoffmann, K. Johnson, C. Kenyon, J. Klaus, B. McIntyre, K. Mistry, A. Murphy, J. Sandford, M. Silberstein, S. Sivakumar, P. Smith, K. Zawadski, S. Thompson and M. Bohr, *IEDM 2003*, section 11.6, p. 98, Dec. 2003.